Mast cell activation and degranulation promotes renal fibrosis in experimental unilateral ureteric obstruction

Shaun A. Summers[1,2], Poh-yi Gan[1], Lakshi Dewage[1], Frank T. Ma[2], Joshua D. Ooi[1], Kim M. O'Sullivan[1], David J. Nikolic-Paterson[2], A. Richard Kitching[1,2] and Stephen R. Holdsworth[1,2]

[1]Centre for Inflammatory Diseases, Department of Medicine, Monash University, Clayton, Victoria, Australia and [2]Monash Medical Centre, Department of Nephrology, Clayton, Victoria, Australia

Progressive renal fibrosis is the final common pathway leading to renal failure irrespective of the initiating cause. Clinical studies of renal fibrosis found that prominent mast cell accumulation correlated with worse outcomes. Mast cells are pluripotent innate immune cells that synthesize and secrete profibrotic mediators. Here we use mast cell–deficient ($Kit^{W\text{-}sh/W\text{-}sh}$) mice to define a functional pathogenic role for these cells in the development of renal fibrosis. Intrarenal collagen deposition was significantly decreased in mast cell–deficient compared to wild-type mice 7 and 14 days after unilateral ureteric obstruction. The intrarenal expression of mRNAs for transforming growth factor-β, α-smooth muscle actin, chemokines, and renal macrophages and $CD4^+$ T cells were also decreased in mast cell–deficient mice. Reconstitution of the mast cell population in mast cell–deficient mice with wild-type bone marrow–derived mast cells restored the pattern and intensity of renal fibrosis to levels seen in wild-type mice following ureteric ligation. Interestingly, the mast cells were recruited, activated, and degranulated within 6 h of ureteric ligation. A mast cell stabilizer that impairs degranulation, disodium chromoglycate, significantly attenuated renal fibrosis following ureteric ligation in wild-type mice. Thus, mast cells promote renal fibrosis and their targeting may offer therapeutic potential in the treatment of renal fibrosis.

Kidney International (2012) **82,** 676–685; doi:10.1038/ki.2012.211; published online 6 June 2012

KEYWORDS: fibrosis; mast cell; renal inflammation; ureteric obstruction

Correspondence: *Stephen R. Holdsworth, Centre for Inflammatory Diseases, Department of Medicine, Monash University, 246 Clayton Road, Clayton, Victoria 3168, Australia. E-mail: Stephen.Holdsworth@monash.edu*

Received 17 August 2011; revised 9 March 2012; accepted 27 March 2012; published online 6 June 2012

Fibrosis is a common final mechanism of organ injury, including chronic kidney disease, where progressive fibrosis is associated with worsening renal function.[1,2] The histological description of renal fibrosis includes: increased interstitial matrix deposition with fibroblast accumulation, the recruitment of inflammatory cells, the loss of tubular architecture, and changes to the surrounding microvasculature.[3] Unilateral ureteric obstruction (UUO) is an experimental model commonly used to study renal interstitial fibrosis and inflammation. Many of the factors driving fibrosis and injury in UUO have also been correlated with human fibrotic kidney disease. These include increased expression of transforming growth factor-β (TGFβ),[4] increased expression of the myofibroblast marker α-smooth muscle actin (αSMA),[5] and the presence of tissue proteases including matrix metalloproteinases (MMPs).[6] Progressive renal injury in UUO is also accompanied by enhanced interstitial leukocyte recruitment with increased numbers of $CD4^+$ T cells,[7] macrophages,[8] and mast cells.[9]

Mast cells have traditionally been linked to immunoglobulin E–mediated hypersensitivity, asthma, and host defense against parasites. While mast cells are well known for their immunoglobulin E Fcε receptors, they are endowed with multiple receptors allowing for the detection and response to numerous pathological insults. These include threats posed by pathogen- and danger-associated molecular patterns. Mast cells are present at strategic locations including skin surfaces and solid organs, where they are located near vessels and nerve endings. This tactical positioning allows them to act as 'sentinels' and first responders of host defense.[10] As well as a diffuse array of surface receptors, mast cells synthesize and secrete chemokines, cytokines, growth factors, and proteases, facilitating leukocyte recruitment and microbial killing.[11] Although they are sparse in solid organs, their unusual capacity to store large quantities of pre-formed molecules, which are released immediately upon degranulation, allows them to mediate inflammation, injury, and repair, despite their limited numbers. In addition to their critical role in host survival from infection,[12,13] the diverse repertoire of functions has resulted in mast cells

being linked with fibrosis, inflammation, and autoimmunity, reviewed recently.[9]

Mice with mutations in *c-kit* expression or signaling are deficient in mast cells; *c-kit* is essential for mast cell differentiation. Historically many experimental studies examining mast cell function *in vivo* used $Kit^{w/W\text{-}v}$ mice. However, while $Kit^{w/W\text{-}v}$ mice contain virtually no mast cells, they display phenotypic abnormalities that are not related to mast cell function. These abnormalities include: macrocytic anemia, sterility, decreased lymphocyte counts, as well as increased rates of dermatitis and gastric pathologies including cancers.[14] More recently, mice where the effects of *c-kit* are more restricted to mast cell deficiency alone, $Kit^{W\text{-}sh/W\text{-}sh}$ mice, have been described and published.[14] $Kit^{W\text{-}sh/W\text{-}sh}$ mice remain equally mast cell deficient; however, they are fertile, have intact immune systems, and are not anemic. These mice have been extensively used to study the role of mast cells *in vivo* and considering the phenotypic similarity to C57BL/6 wild-type (WT) mice and are recommended for studying the physiological function of mast cells *in vivo*.[14] $Kit^{W\text{-}sh/W\text{-}sh}$ mice have been used to explore the role of mast cells in acute kidney injury[15] and chronic glomerulonephritis.[16] Although additional factors could influence outcome results observed in $Kit^{w/W\text{-}v}$ mice compared with mast cell-intact WT, changes seen in $Kit^{W\text{-}sh/W\text{-}sh}$ mice can be more accurately attributed to mast cell deficiency. These observations can be confirmed when $Kit^{W\text{-}sh/W\text{-}sh}$ mice are reconstituted with mast cells from WT mice and the patterns and severity of injury are comparable to those seen in WT mice. Reconstitution of $Kit^{W\text{-}sh/W\text{-}sh}$ mice with bone marrow–derived mast cells from WT mice results in normal numbers and function of mast cells,[14] including in the resting and diseased kidney.[16]

Mast cells are associated with a variety of renal diseases and increased mast cell accumulation correlates with disease severity and poorer outcome in chronic inflammation and fibrosis (reviewed by Holdsworth and Summers[9] and Mack and Rosenkranz[17]). Experimentally mast cells demonstrate both inflammatory[16,18] and protective functions[19–21] in the kidney, which consistent with the diverse array of mediators released. The role of mast cells in progressive kidney fibrosis is less clearly defined. The correlation of mast cells with injury and fibrosis suggests that they are mechanistically linked to progressive fibrosis, although a pathogenic functional role is not established. Mast cells contain an array of potentially profibrotic mediators that include: chemokines, growth factors (including TGFβ), leukotrienes, and proteases (including MMP3, MMP9, and MMP12),[22,23] which could enhance renal fibrosis. Potentially mast cell activation and degranulation could result in the release of inflammatory and profibrotic mediators promoting renal fibrosis and injury.

In this paper, we have defined a role for mast cells in renal fibrosis induced by UUO. At 7 days after UUO, hydronephrotic kidneys from WT mice had developed increased collagen deposition, amplified expression of TGFβ, αSMA, and MMP12, and enhanced leukocyte recruitment. Mast cell–deficient, $Kit^{W\text{-}sh/W\text{-}sh}$ mice were protected from fibrotic injury induced by UUO. Similarly, 14 days after ureteric ligation, protection persisted in the absence of mast cells, with significantly decreased intrarenal collagen and αSMA deposition in the hydronephrotic kidneys of $Kit^{W\text{-}sh/W\text{-}sh}$ mice. Furthermore, when UUO was performed on $Kit^{W\text{-}sh/W\text{-}sh}$ mice, which had been reconstituted with bone marrow–derived mast cells from WT mice, the pattern and severity of histological renal injury seen in $Kit^{W\text{-}sh/W\text{-}sh}$ mice was similar to that observed in WT mice, demonstrating that mast cells were directly pathogenic and profibrotic. Pre-emptive treatment with sodium chromoglycate, a mast cell stabilizer, protected WT mice from fibrosis and renal injury. These results demonstrate that mast cells with their pro-inflammatory mediators enhance renal fibrosis, leukocyte recruitment, and injury after UUO.

RESULTS

Seven days after UUO, mast cell–deficient $Kit^{W\text{-}sh/W\text{-}sh}$ mice have decreased renal fibrosis

The development of fibrosis in the hydronephrotic kidney is characterized by the deposition of collagen and αSMA in the renal interstitium. We assessed renal collagen deposition after picrosirius red staining, which was then analyzed using NIH image analysis. Collagen deposition was increased in both WT and $Kit^{W\text{-}sh/W\text{-}sh}$ mice compared to untreated WT mice (dotted line, mean = 2.4 ± 0.4%). Compared to WT mice collagen deposition was significantly decreased in $Kit^{W\text{-}sh/W\text{-}sh}$ mice 7 days after UUO (Figure 1a). Representative photomicrographs of the renal interstitium in WT and $Kit^{W\text{-}sh/W\text{-}sh}$ mice after picrosirius red staining are demonstrated in color as viewed under polarized light (Figure 1b and c), in black and white (Figure 1d and e), and after NIH image analysis (Figure 1f and g). Interstitial αSMA deposition was also decreased in $Kit^{W\text{-}sh/W\text{-}sh}$ mice compared to WT mice after NIH image analysis (Figure 2). In untreated WT mice, αSMA deposition was consistently measured at $<1\%$. Representative images demonstrating decreased αSMA staining in color (Figure 2b and c), black and white (Figure 2d and e), and after analysis (Figure 2f and g) in $Kit^{W\text{-}sh/W\text{-}sh}$ mice are shown.

Mast cells are recruited to hydronephrotic kidneys after UUO, where they are activated and degranulated

Mast cells were easily detected in the lymph nodes of WT mice (Figure 3a), while they were not seen in lymph nodes or kidneys of $Kit^{W\text{-}sh/W\text{-}sh}$ mice. Although infrequently observed, mast cells were seen in the kidneys of WT mice, 7 days after UUO (Figure 3b), after methyl Carnoy's fixation and toluidine blue staining. The serine protease chymase, which is produced exclusively by mast cells and basophils, was readily detected in the hydronephrotic kidneys of WT mice, while levels of expression were at or below the lowest level of detection in hydronephrotic kidneys from $Kit^{W\text{-}sh/W\text{-}sh}$ mice (Figure 3c); values were normalized to 1 in the hydronephrotic kidneys of WT mice. The presence of mast cells and the expression of chymase, a mast cell degranulation product, provide evidence that mast cell activity was present in the hydronephrotic kidneys of WT mice, even after 7 days.

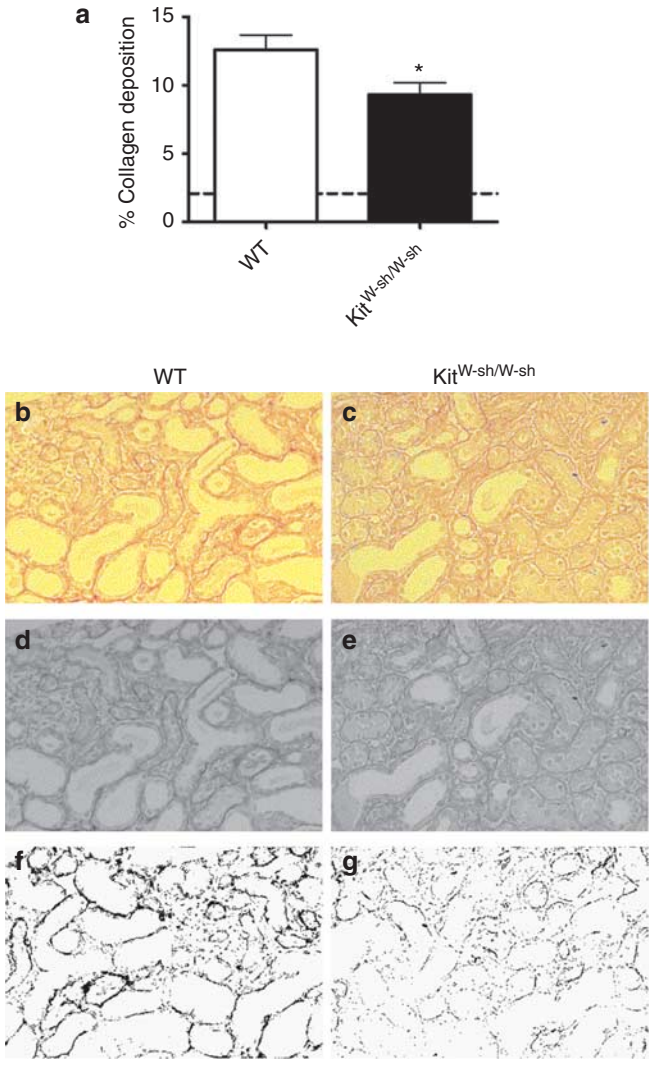

Figure 1 | Renal fibrosis is decreased in mast cell–deficient ($Kit^{W\text{-}sh/W\text{-}sh}$) mice. At 7 days after unilateral ureteric obstruction (UUO), there was less interstitial collagen deposition (**a**) in the kidneys of $Kit^{W\text{-}sh/W\text{-}sh}$ mice ($n = 8$) compared to (C57BL/6) wild-type (WT) mice ($n = 9$). Photomicrographs of collagen deposition in WT and $Kit^{W\text{-}sh/W\text{-}sh}$ mice after picrosirius red (PSR) staining are shown. Representative kidney sections visualized in color, viewed under polarized light, at original magnification $\times 400$ in (**b**) WT and (**c**) $Kit^{W\text{-}sh/W\text{-}sh}$ mice are shown, (**d**, **e**) in black and white, and (**f**, **g**) after NIH image analysis. The dotted line represents the mean collagen deposition in untreated WT mice. $^*P < 0.05$.

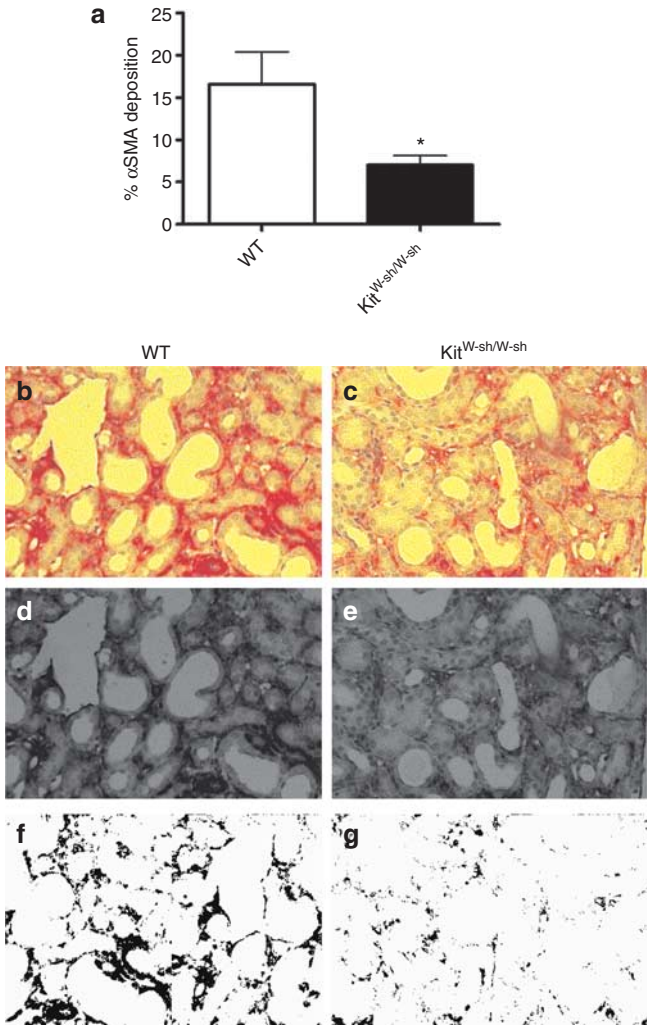

Figure 2 | The deposition of α-smooth muscle actin (αSMA) is decreased in the absence of mast cells. (**a**) The deposition of αSMA was significantly decreased in the hydronephrotic kidneys of $Kit^{W\text{-}sh/W\text{-}sh}$ mice ($n = 8$) compared to the hydronephrotic kidneys of wild-type (WT) mice ($n = 9$). Representative kidney sections demonstrating αSMA deposition in (**b**) WT and (**c**) $Kit^{W\text{-}sh/W\text{-}sh}$ mice visualized in color, viewed under polarized light, (**d**, **e**) in black and white, and (**f**, **g**) after NIH image analysis are shown. In untreated WT mice, αSMA deposition was measured at $< 1\%$. All images are shown at original magnification $\times 400$. $^*P < 0.05$.

We hypothesized that mast cells were recruited to the kidneys early in the disease process. To assess mast cell activation (and degranulation), we performed UUO on WT mice and assessed kidney tryptase production at time zero and in the hydronephrotic kidneys at 6 h, 48 h, and 1 week after ureteric ligation (Figure 3d). We found that mast cell activation peaked 6 h after ureteric ligation, and tryptase remained elevated after 48 h (5.2 ± 1.2 ng/ml of tryptase) and then decreased. At 1 week after UUO, kidney tryptase production had fallen to similar levels recorded in untreated WT mice.

To demonstrate conclusively mast cell recruitment to hydronephrotic kidneys, we labeled mast cells with a cell tracker and injected them into $Kit^{W\text{-}sh/W\text{-}sh}$ mice, which lack any endogenous mast cells. We then performed ureteric ligation and assessed kidney mast cell accumulation, 6 h later. Mast cells were readily detected in the hydronephrotic kidneys of injected $Kit^{W\text{-}sh/W\text{-}sh}$ mice after green staining (Figure 3e). Mast cells were not present in the contralateral kidney (Figure 3f).

After ureteric ligation, kidney production and expression of profibrotic growth factors were decreased in the absence of mast cells

At 7 days after UUO, we measured TGFβ production from homogenized hydronephrotic kidneys of WT and $Kit^{W\text{-}sh/W\text{-}sh}$

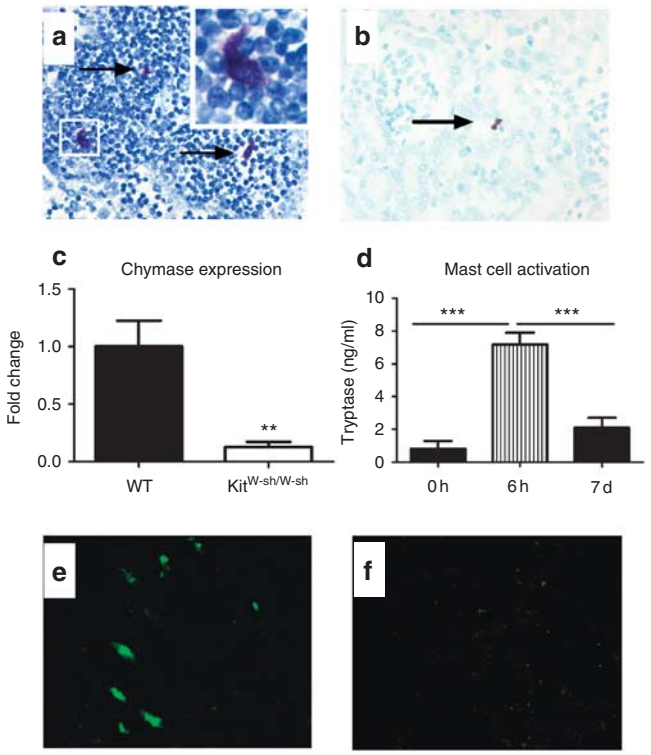

Figure 3 | Mast cells were present in the kidneys of hydronephrotic wild-type (WT) mice. (**a**) After toluidine blue staining, mast cells were seen in the lymph nodes of untreated WT mice at original magnification $\times 400$, demonstrated by the arrow heads and in the white box (original magnification $\times 1200$). (**b**) After fixation with methyl Carnoy's solution and staining with toluidine blue, mast cells were seen (occasionally) in the hydronephrotic kidneys of WT mice, 7 days after unilateral ureteric obstruction (UUO). At 7 days after UUO, chymase was detected in the hydronephrotic kidneys of WT mice ($n = 9$), and the expression was normalized to 1 in the hydronephrotic kidney of WT mice. (**c**) Low levels of chymase expression were detected in the hydronephrotic kidneys of Kit$^{W\text{-}sh/W\text{-}sh}$ mice ($n = 8$). (**d**) Compared to untreated WT mice ($n = 6$), mast cell activation and degranulation peaked after 6 h ($n = 4$) and then decreased, approaching baseline levels after 7 days ($n = 4$). Subsequently, we labeled mast cells with a cell tracker and injected them into Kit$^{W\text{-}sh/W\text{-}sh}$ mice ($n = 4$). We then performed ureteric ligation and assessed mast cell accumulation 6 h later. (**e**) Mast cells (green) were readily identified in the hydronephrotic kidneys, but were not seen in the (**f**) contralateral, control kidney, original magnification $\times 400$. $^{**}P < 0.01$, $^{***}P < 0.001$.

mice. While TGFβ production was increased in both groups of experimental mice, compared to controls (where it was undetectable), it was decreased in Kit$^{W\text{-}sh/W\text{-}sh}$ mice, compared to WT mice (Figure 4a). There was also a significant increase in intrarenal mRNA expression of TGFβ, αSMA, MMP3, and MMP12 in the hydronephrotic kidneys of WT and Kit$^{W\text{-}sh/W\text{-}sh}$ mice compared to control kidneys (levels of expression in untreated WT mice are represented by the dotted line). After UUO, kidney expression of TGFβ (Figure 4b), αSMA (Figure 4c), and MMP12 (Figure 4d) was decreased in Kit$^{W\text{-}sh/W\text{-}sh}$ mice compared to WT mice, while there was no change in MMP2, MMP3, and MMP9 expression (Figure 4e–g). The association of enhanced collagen and myofibroblast deposition with increased kidney expression of profibrotic markers highlighted a potential pathogenic role for mast cells in the initiation and progression of renal fibrosis.

Seven days after UUO, kidney chemokine expression and interstitial leukocyte recruitment were decreased in Kit$^{W\text{-}sh/W\text{-}sh}$ mice

We assessed the intrarenal expression of key leukocyte chemoattractants. Intrarenal mRNA expression of chemokine ligands (Figure 5a), which are chemoattractants for monocytes CCL5 and T cells (CXCL9, CXCL10, and CCL20) were all decreased in Kit$^{W\text{-}sh/W\text{-}sh}$ mice. Assessing the neutrophil-attracting chemokines, we found that CXCL2 expression was reduced, while CXCL1 expression was unaltered between experimental groups. Subsequently, we found that renal interstitial macrophage and CD4$^+$ T cell recruitment was significantly decreased in Kit$^{W\text{-}sh/W\text{-}sh}$ mice compared to WT mice, while neutrophil recruitment was equivalent (Figure 5b–d and Supplementary Figure S1 online). These results demonstrated that mast cells enhance the local production of chemokines and leukocyte recruitment after ureteric ligation.

Fourteen days after UUO, fibrosis is significantly attenuated in the absence of mast cells

To determine if the protection in fibrosis observed in the absence of mast cells persisted after the first week, we performed ureteric ligation in WT and Kit$^{W\text{-}sh/W\text{-}sh}$ mice and examined fibrosis in the hydronephrotic kidneys, 14 days later. We found that intrarenal collagen deposition measured after picrosirus red staining was decreased in the absence of mast cells (Figure 6a). Similarly, αSMA deposition and expression (Figure 6b and c) was decreased in the hydronephrotic kidneys of Kit$^{W\text{-}sh/W\text{-}sh}$ mice compared to hydronephrotic kidneys from WT mice. There was no difference in intrarenal TGFβ expression between the two groups (WT 1.0 ± 0.3 vs. Kit$^{W\text{-}sh/W\text{-}sh}$ mice 0.7 ± 0.1-fold), and values were normalized to 1 in the hydronephrotic kidneys of WT mice.

Mast cell reconstitution restored the severity of fibrotic injury in Kit$^{W\text{-}sh/W\text{-}sh}$ mice

To confirm that the decreased fibrosis observed in Kit$^{W\text{-}sh/W\text{-}sh}$ mice was a direct consequence of mast cell deficiency, we reconstituted Kit$^{W\text{-}sh/W\text{-}sh}$ mice with bone marrow–derived mast cells from WT mice. Successful reconstitution was confirmed after demonstrating mast cells in the lymph nodes and kidneys of mast cell–transplanted mice, as published previously.[15] After 12 weeks, when reconstitution was complete, we performed UUO on mast cell–reconstituted Kit$^{W\text{-}sh/W\text{-}sh}$ mice and age-matched mast cell–deficient Kit$^{W\text{-}sh/W\text{-}sh}$ mice. We assessed renal fibrosis and injury 7 days later.

Reconstitution of Kit$^{W\text{-}sh/W\text{-}sh}$ mice with mast cells from WT mice followed by ureteric ligation resulted in a pattern and severity of renal injury similar to that seen in hydronephrotic kidneys of WT mice. Extracellular matrix

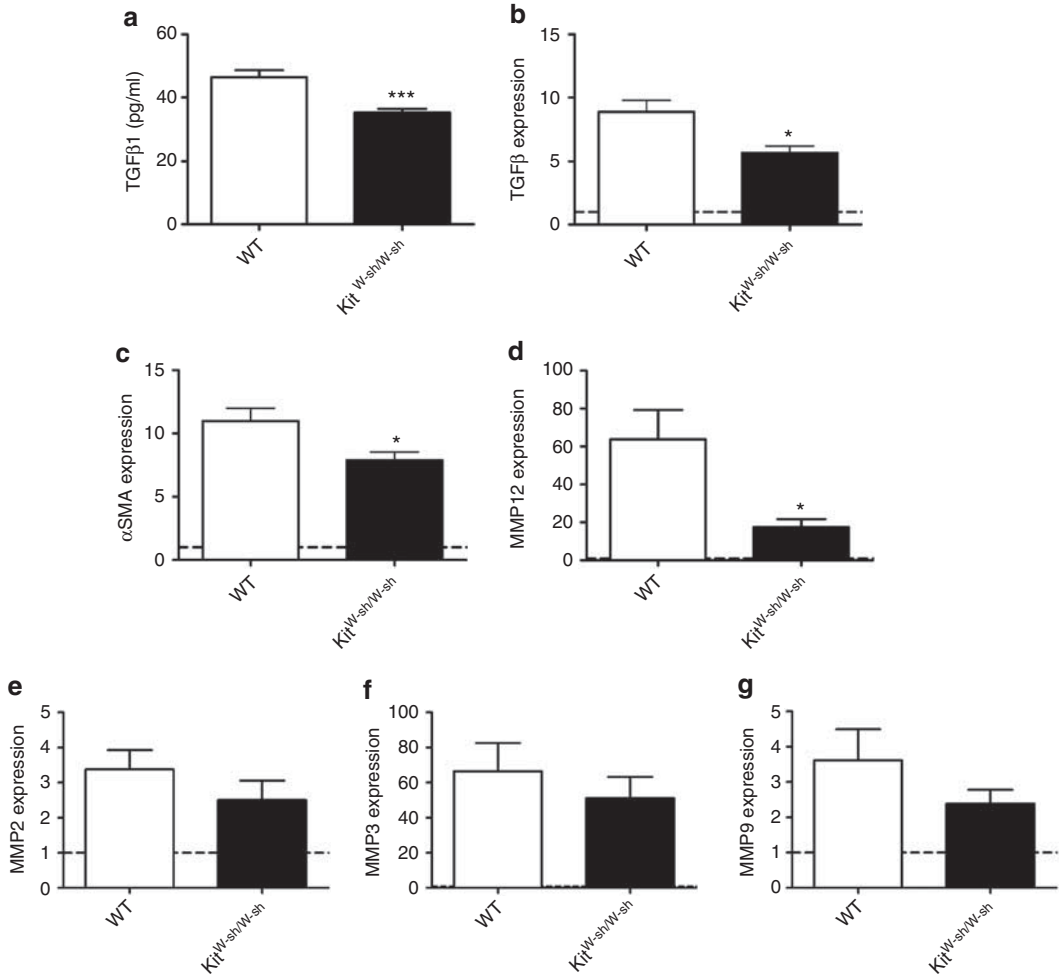

Figure 4 | The expression and production of profibrotic markers were decreased in hydronephrotic kidneys from Kit$^{W\text{-}sh/W\text{-}sh}$ mice. (**a**) At 7 days after unilateral ureteric obstruction (UUO), production of transforming growth factor-β (TGFβ) was highly significantly decreased in the hydronephrotic kidneys of Kit$^{W\text{-}sh/W\text{-}sh}$ mice ($n = 8$) compared to hydronephrotic wild-type (WT) kidneys ($n = 9$). (**b**–**d**) Similarly, mRNA expression levels of TGFβ, α-smooth muscle actin (αSMA), and matrix metalloproteinase 12 (MMP12) were all decreased in the hydronephrotic kidneys of Kit$^{W\text{-}sh/W\text{-}sh}$ mice compared to WT mice. (**e**–**g**) There was no difference in the MMP2, MMP3, or MMP9 kidney expression between the two experimental groups. The dotted line represents the mean value recorded in untreated WT mice. *$P < 0.05$, ***$P < 0.001$.

deposition was increased in reconstituted Kit$^{W\text{-}sh/W\text{-}sh}$ mice compared to control, un-reconstituted Kit$^{W\text{-}sh/W\text{-}sh}$ mice (Figure 7a). Representative black and white (Figure 7b and c) and NIH image analyzed (Figure 7d and e) photomicrographs demonstrate this result. Consistent with this finding, we demonstrated a trend of increase in intrarenal TGFβ expression ($P = 0.08$), while αSMA expression was significantly increased in reconstituted Kit$^{W\text{-}sh/W\text{-}sh}$ mice (Figure 7f and g). These studies provide direct evidence that mast cells augment renal fibrosis after UUO.

Disodium chromoglycate, a mast cell stabilizer, decreased renal fibrosis in UUO

Disodium chromoglycate is a commonly used therapeutic agent, which impairs mast cell degranulation. To test the therapeutic potential of DSCG in limiting renal fibrosis, we administered DSCG or control, sterile saline, to WT mice 2 days before ureteric ligation and then on alternate days until experiments ended (day 7). Administration of DSCG to WT mice resulted in decreased extracellular matrix deposition (Figure 8a–e) compared to WT mice treated with control. Furthermore, there was a decrease in intrarenal TGFβ and αSMA expression in mice treated with DSCG (Figure 8f and g). These results confirmed the role of mast cell degranulation in promoting renal fibrosis and highlighted the therapeutic potential of DSCG in the treatment of renal fibrosis.

DISCUSSION

Mast cells have been implicated in several different types of kidney disease. Numerically mast cell accumulation correlates positively with increased renal injury and decreased function in immunoglobulin A nephropathy, diabetic nephropathy, allograft rejection, amyloidosis, renovascular disease,

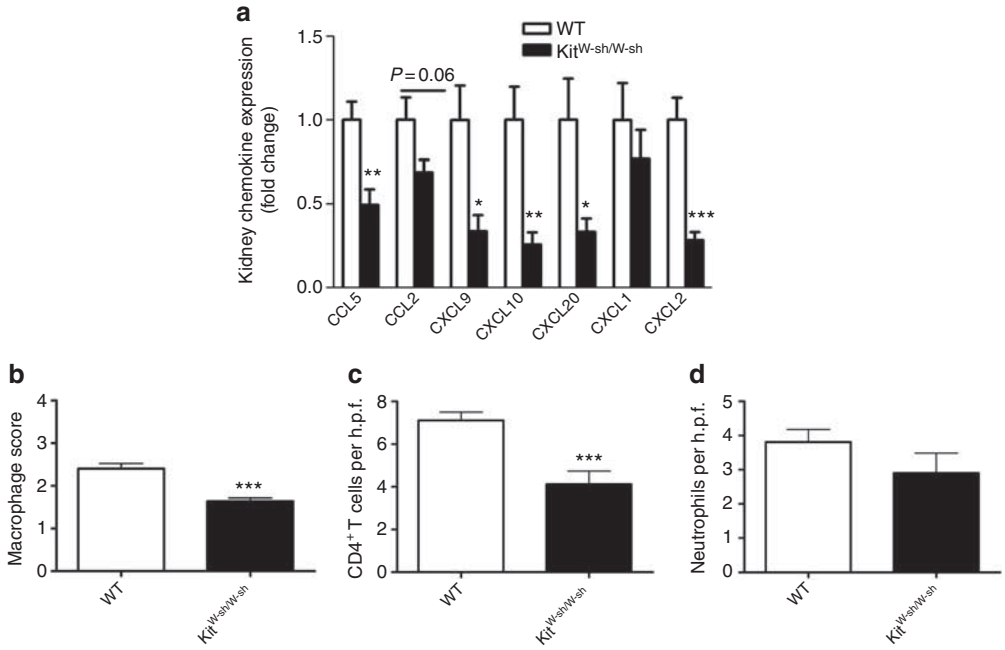

Figure 5 | Chemokine expression and leukocyte recruitment was decreased in Kit$^{W\text{-}sh/W\text{-}sh}$ mice. (**a**) Kidney expression of key monocyte (CCL5), CD4$^+$ T cell (CXCL9, CXCL10, and CCL20) and neutrophil (CXCLR2) was decreased in Kit$^{W\text{-}sh/W\text{-}sh}$ mice ($n = 8$) compared to WT mice ($n = 9$). There was a significant decrease in (**b**) interstitial macrophage and (**c**) CD4$^+$ T cell recruitment in Kit$^{W\text{-}sh/W\text{-}sh}$ mice, while (**d**) neutrophil recruitment was unchanged between the two experimental groups. *$P < 0.05$, **$P < 0.01$, ***$P < 0.001$.

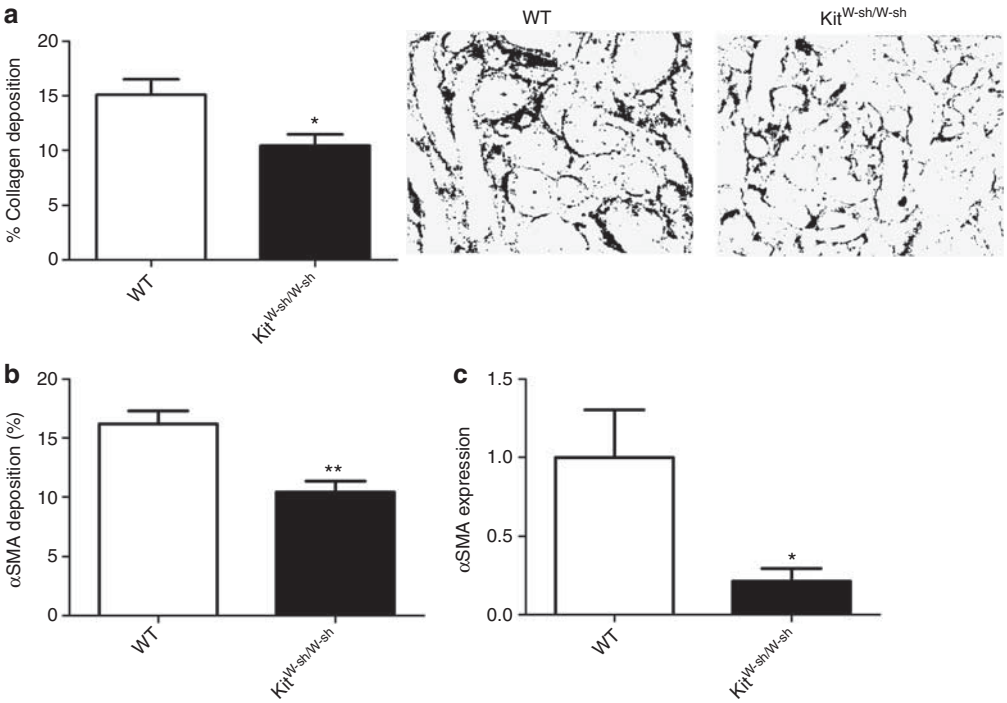

Figure 6 | Renal fibrosis is decreased in mast cell–deficient (Kit$^{W\text{-}sh/W\text{-}sh}$) mice, 14 days after ureteric ligation. (**a**) Compared to wild-type (WT) mice ($n = 10$), collagen deposition, assessed after picrosirius red staining and NIH image analysis, was decreased in Kit$^{W\text{-}sh/W\text{-}sh}$ ($n = 9$) mice. Representative images of fibrosis after NIH image analysis from WT and Kit$^{W\text{-}sh/W\text{-}sh}$ mice are shown. (**b**) Kidney production and (**c**) expression of α-smooth muscle actin (αSMA) was also decreased in the absence of mast cells. *$P < 0.05$, **$P < 0.01$.

polycystic kidney disease, and drug-induced nephritis.[9] Experimental studies have largely been confirmatory, linking mast cell numbers and staining intensity with increased TGFβ production and interstitial fibrosis.[9,17,24,25] These studies suggest that mast cells are associated with the development of renal fibrosis; however, a causal relationship

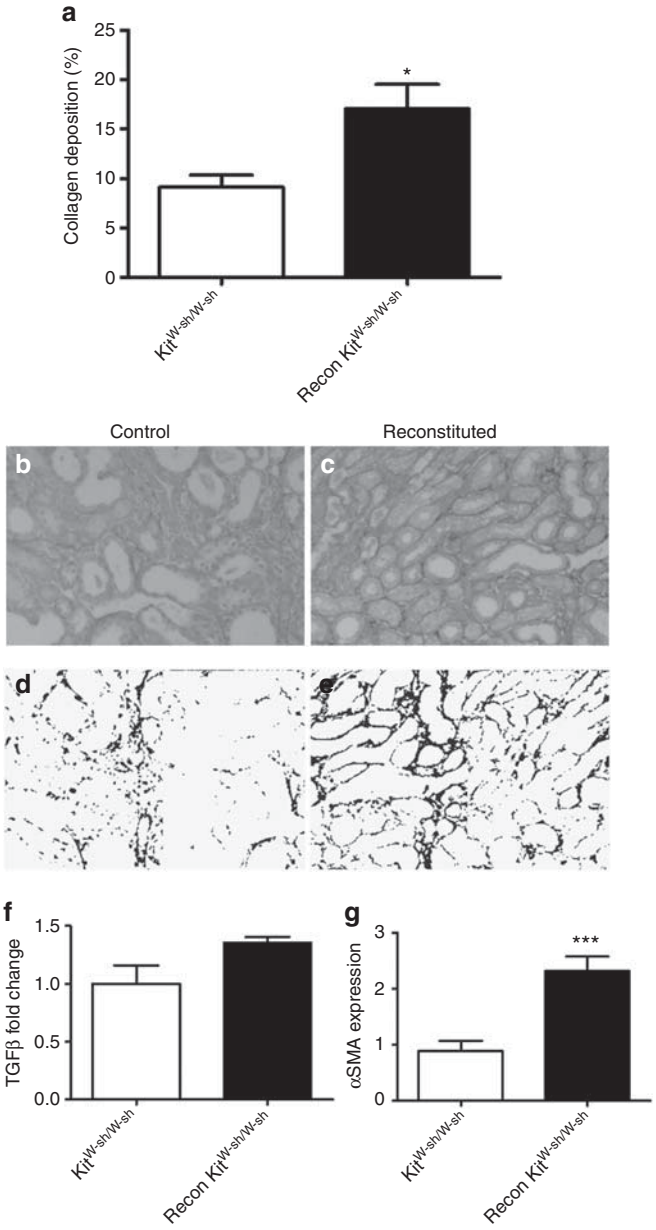

Figure 7 | Mast cells promote renal fibrosis. To assess the direct pathogenicity of mast cells, we reconstituted $Kit^{W\text{-}sh/W\text{-}sh}$ mice with bone marrow–derived mast cells from wild-type (WT) mice. When reconstitution was complete, after 12 weeks, we performed unilateral ureteric obstruction (UUO) on reconstituted $Kit^{W\text{-}sh/W\text{-}sh}$ mice ($n = 7$), and age-matched $Kit^{W\text{-}sh/W\text{-}sh}$ mice ($n = 8$) that were not reconstituted served as controls. We assessed renal fibrosis 7 days later. (**a**) Collagen deposition was increased in reconstituted $Kit^{W\text{-}sh/W\text{-}sh}$ mice compared to control $Kit^{W\text{-}sh/W\text{-}sh}$ mice. Representative photomicrographs of the hydronephrotic kidneys after PSR staining of (**b**, **d**) control $Kit^{W\text{-}sh/W\text{-}sh}$ mice and (**c, e**) reconstituted $Kit^{W\text{-}sh/W\text{-}sh}$ mice are shown in black and white and after NIH image analysis. (**f, g**) Kidney mRNA expression of TGFβ showed a trend of increase, while α-smooth muscle actin (αSMA) expression was highly significantly increased in the kidneys of reconstituted $Kit^{W\text{-}sh/W\text{-}sh}$ mice. All images are shown at original magnification × 400. $^{*}P < 0.05$, $^{***}P < 0.001$.

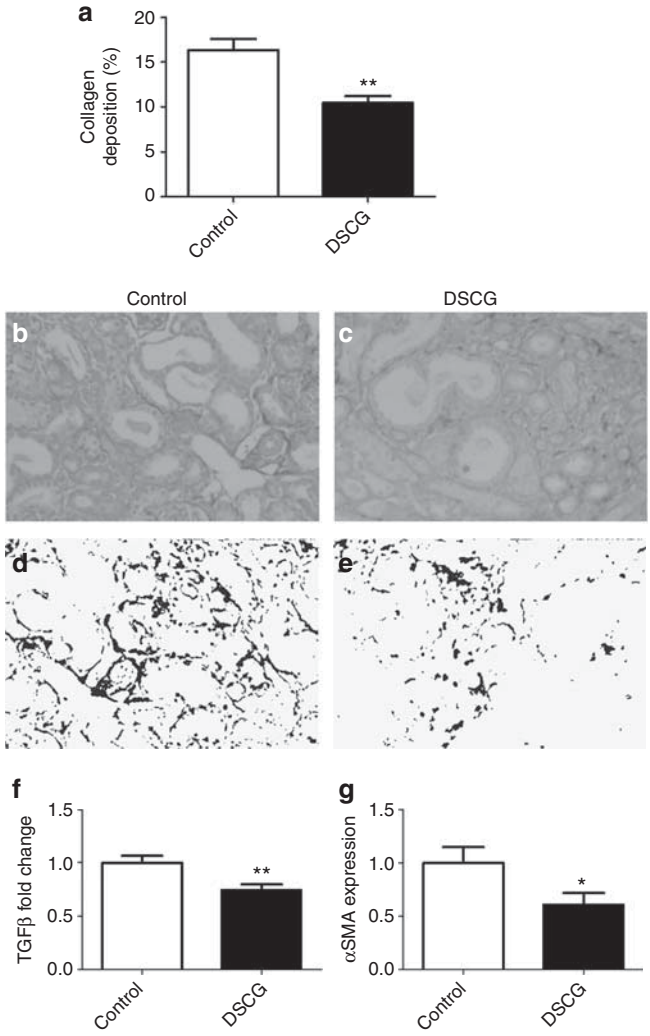

Figure 8 | Mast cell stabilization attenuated renal fibrosis. To assess the clinical effect of mast cell stabilization, we pre-emptively administered disodium chromoglycate (DSCG) ($n = 10$) or control (sterile saline) ($n = 10$) to wild-type (WT) mice and then performed unilateral ureteric obstruction (UUO). (**a**) Mice treated with DSCG had decreased collagen deposition in their kidneys. Representative kidney sections demonstrating collagen deposition in (**b**, **d**) control and (**c**, **e**) DSCG-treated mice are shown. Intrarenal mRNA expression of (**f**) TGFβ and (**g**) α-smooth muscle actin (αSMA) was decreased after treatment with DSCG. All images are shown at original magnification × 400. $^{*}P < 0.05$, $^{**}P < 0.01$.

is not established. In this paper, we demonstrate a direct pathogenic role for mast cells in the promotion of renal interstitial fibrosis induced by UUO. Evidence for a direct pathogenic role for mast cells is strong and comes from three lines of experimental data. Firstly, mast cell–deficient mice develop less renal fibrosis compared to mast cell–replete mice. This attenuation in fibrosis observed in $Kit^{W\text{-}sh/W\text{-}sh}$ extended to 14 days after UUO. A direct role for mast cells was confirmed when the mast cell population was reconstituted in mast cell–deficient mice and injury levels were similar to those observed in WT mice after UUO. Finally, we

demonstrated that inhibition of mast cell degranulation with DSCG diminished renal fibrotic injury.

Mast cells contain a variety of bioactive mediators, including growth factors, proteases, leukotrienes, cytokines, and chemokines, many of these could potentially promote fibrosis. Direct evidence that mast cells could increase collagen deposition and fibrosis was first demonstrated nearly two decades ago in a dermal hypersensitivity model. In this model, mast cell activation stimulated TGFβ production from skin fibroblasts, which resulted in increased collagen deposition.[26] The pleiotropic cytokine, TGFβ, has diverse physiological roles *in vivo* including initiation and control of fibrosis.[27] The profibrotic effects of mast cells are intricately linked with TGFβ. Mast cells produce,[26,28] and activate TGFβ, through the production of chymase.[29] Interestingly, TGFβ is also a potent mast cell chemoattractant.[30,31] This self-perpetuating profibrotic cycle helps explain the diminution in renal injury we observed in mast cell–deficient mice after UUO. In $Kit^{W\text{-}sh/W\text{-}sh}$ mice, decreased fibrosis was accompanied by less intrarenal TGFβ production, while TGFβ and chymase mRNA expression was also significantly decreased. The full pattern of injury and expression of fibrosis returned when the mast cell population was successfully reconstituted. In addition to TGFβ and chymase production, mast cells contain other pre-formed mediators that can induce fibrosis. In clinical studies, mast cell degranulation products, including tryptase, positively correlate with advancing renal injury in chronic kidney disease.[32] Mast cells also contain MMP3, MMP9, and MMP12,[22,23] which have been implicated in renal fibrosis.[3] In experimental lung disease, MMP12 is upregulated and promotes macrophage recruitment and fibrosis.[33] In our studies, MMP12 was decreased in $Kit^{W\text{-}sh/W\text{-}sh}$ mice, consistent with decreased renal fibrosis. Mast cell degranulation results in the rapid release of these mediators that are likely to promote fibrosis. Confirmatory and mechanistic proof for a pathogenic role for mast cell degranulation was demonstrated when we pre-emptively treated mice with DSCG. Administering the mast cell stabilizer attenuated renal fibrosis and decreased kidney TGFβ and αSMA expression. Disodium chromoglycate has been shown to have mast cell specificity, and in a model of endotoxemic sepsis, administration of DSCG exclusively decreased serum tumor necrosis factor levels and survival in WT mice (this effect was not seen in mast cell–deficient mice treated with DSCG).[34]

Few mast cells were seen in the hydronephrotic kidneys of WT mice, 1 week after UUO. While intrarenal chymase expression was detectable in the hydronephrotic kidneys 1 week after ureteric ligation, levels were similar to those seen in untreated WT mice. Therefore, we assessed mast cell accumulation and activation (tryptase production) early after UUO. Consistent with their function as first responders to inflammation and injury, we found that mast cells were recruited and activated (degranulated) and released pro-inflammatory mediators in the kidney within 6 h of ureteric ligation. Kidney mast cell activity had significantly decreased 1 week after UUO and returned to levels seen in untreated WT mice. Despite their early recruitment to the injured kidney, the pathological profibrotic properties of mast cells persist to (at least) 14 days, when fibrosis is attenuated in the absence of mast cells.

In response to stress, mast cells degranulate and secrete chemokines and cytokines that recruit leukocytes to areas of inflammation that are required for host defense.[12,13] In UUO, leukocyte recruitment is increased and positively correlates with renal fibrosis.[35] Macrophages[36] and $CD4^+$ T cells[7] have been associated with progressive renal injury after UUO. We found that intrarenal chemokine expression of CCL5 was decreased with a trend of decrease in CCL2 expression in $Kit^{W\text{-}sh/W\text{-}sh}$ mice compared to WT mice after UUO. This was associated with decreased interstitial macrophage recruitment. Similarly, intrarenal expression of CXCL9 and CXCL10, two key Th1-attracting chemokines and CCL20, a key Th17-attracting chemokine, was decreased in $Kit^{W\text{-}sh/W\text{-}sh}$ mice. Decreased chemokine expression correlated with fewer $CD4^+$ T cells observed in the renal interstitium. These data add credence to the hypotheses that after stress mast cell degranulate and release chemokines. Increased chemokine production results in the recruitment of pro-inflammatory leukocytes that contribute to the development of renal fibrosis.

In both clinical and experimental studies, mast cells have been shown to be profibrotic. Clinically this is well demonstrated in lung fibroblasts,[37] stenotic heart valves,[38] and tumors,[39] while experimentally this has been validated in the skin,[40] hepatic,[41] and cardiac fibrosis[42] models. While mast cell accumulation correlates with deteriorating renal function, a previous study examining the role of mast cells in renal fibrosis did not find them to be pathogenic.[43] These authors observed increased fibrosis in $Kit^{w/W\text{-}v}$ mice after UUO. Interestingly, they found enhanced leukocyte recruitment (with intact chemokine expression) in the $Kit^{w/W\text{-}v}$ mice. These results conflict with our findings of decreased fibrosis, decreased chemokine expression, and decreased interstitial leukocyte recruitment in $Kit^{W\text{-}sh/W\text{-}sh}$ mice. Our results are consistent with the physiological effects usually attributed to mast cells. The most likely explanation for the discrepancy in results rests with the multiple additional phenotypic abnormalities seen in $Kit^{w/W\text{-}v}$ mice, which are not a result of mast cell deficiency. Similar discrepancies in results have been reported in experimental arthritis, where protection afforded to $Kit^{w/W\text{-}v}$ mice was not transferred to $Kit^{W\text{-}sh/W\text{-}sh}$ mice, a likely consequence of the hematological and immunological abnormalities consistently observed in $Kit^{w/W\text{-}v}$ mice.[44]

In conclusion, we have provided definitive proof that mast cell activation and degranulation promotes renal fibrosis. Mast cells are recruited early to the obstructed kidney, where they are activated; they release profibrotic factors and chemokines, which subsequently recruit pro-inflammatory leukocytes. This heightened inflammatory state results in enhanced fibrosis, which persists for at least 2 weeks after ureteric ligation. Inhibition of mast cell degranulation, with

DSCG, diminished fibrosis and injury highlighting the therapeutic potential of targeting mast cells in the treatment of renal fibrosis.

MATERIALS AND METHODS

Experimental design and statistical analyses

The 8- to 10-week-old male WT (C57BL/6) and $Kit^{W\text{-}sh/W\text{-}sh}$ mice were used in all experiments. WT mice were purchased from Monash University Animal Services (Melbourne, Victoria, Australia). $Kit^{W\text{-}sh/W\text{-}sh}$ mice were purchased from Jackson Laboratories (Bar Harbor, ME) and bred at Monash University. Studies adhered to the National Health and Medical Research Council of Australia guidelines for animal experimentation. The left ureter was ligated under general anesthesia and renal injury and fibrosis was studied after: 6 h, 48 h, 7 days, or 14 days, as described previously.[45] Disodium chromoglycate (Sigma-Aldrich, St Louis, MO) at a dose of 10 mg/kg was dissolved in sterile saline and injected at day −2 and then on alternate days for the duration of experiments. Control mice were injected with equivalent volumes of sterile saline. Data are expressed as mean ± s.e.m. Data were analyzed using Student's *t*-test and GraphPad Prism (GraphPad Software, San Diego, CA). A *P*-value of <0.05 was considered significant.

Assessment of renal fibrosis and interstitial macrophage, $CD4^+$, and neutrophil staining

For assessment of fibrosis, kidney sections were fixed in Bouin's fixative and embedded in paraffin. Tissue sections (3 μm tissue) from all mice were stained with picrosirius red (Sigma-Aldrich). Collagen deposition was assessed under polarized light and quantitated by NIH image analysis (Scion Image, Scion Corporation, Frederick, MD). A minimum of 10 low-power (× 100) fields were assessed per animal, covering the whole kidney, while vascular, periglomerular, and perivascular areas were excluded. Results are expressed as the percentage of interstitial cortical area affected. For assessment of αSMA deposition, we used αSMA 1A4mAb (DAKO, Glostrup Denmark), followed by a rabbit anti-mouse biotinylated secondary antibody (DAKO), streptavidin alkaline phosphatase (DAKO), and visualized by a red alkaline phosphatase substrate kit (Vector Laboratories, Burlingame, CA). For leukocyte staining, kidney sections were fixed in periodate lysine paraformaldehyde for 4 h, and then washed with 20% sucrose solution and frozen in liquid nitrogen. Tissue sections were cut and a three-layered immunoperoxidase technique was used to stain for macrophages, T cells, and neutrophils. The primary antibodies used were: FA/11 for macrophages GK1.5 (anti-mouse CD4; American Type Culture Collection (ATCC), Manassas, VA) and RB6-8C5 (anti-Gr-1; DNAX, Palo Alto, CA) for neutrophils. The secondary antibody used was rabbit anti-rat biotin (BD Bioscience, North Ryde, Australia) visualized with 3,3′-diaminobenzidine (Sigma-Aldrich). A minimum of 20 consecutive interstitial sections were assessed per animal and results are expressed as cells per high-power field for neutrophils and $CD4^+$ T cells.[46] For assessment of interstitial macrophage recruitment, we used a previously published scoring system reflecting the area covered by macrophages (1, 0–25%; 2, 26–50%; 3, 51–75%; and 4, 76–100%).[47]

Measurement of kidney TGFβ production and intrarenal mRNA expression of chemokines and cytokines

For measurement of kidney TGFβ production, sections of hydronephrotic kidneys from both groups of experimental mice were digested in 1% cetyl trimethylammonium bromide and phosphate-buffered saline for 2 h at room temperature. Samples were centrifuged at 20,000 *g*. Supernatants were extracted and measured using an enzyme-linked immunosorbent assay (R&D Systems, Minneapolis, MN) according to the manufacturer's protocol. For measurement of RANTES/CCL5, MCP1/CCL2, MIG/CXCL9, IP10/CXCL10, LARC/CCL20, KC/CXCL1, and MIP2/CXCL2, MMP2, MMP3, MMP9, MMP12, TGFβ, and αSMA, RNA was extracted from the kidney and measured by real-time PCR, using techniques and primers we have described previously.[8,46] To measure chymase expression, we used a Taqman Gene Expression Array (Mm00487938_m1; Applied Biosystems, Melbourne, Victoria, Australia). Expression was standardized to 18S (housekeeping gene) before being expressed as a fold increase (or decrease) relative to control.

Assessment of mast cell activation and degranulation

We performed unilateral ureteric ligation on WT mice and removed the hydronephrotic kidneys after 6 h ($n=4$), 48 h ($n=4$), and after 1 week ($n=4$), and for controls we used untreated WT mice ($n=6$). Kidneys were digested with collagenase and DNAse (both Roche Diagnostics, Indianapolis, IN), incubated, and then centrifuged at 13,000 r.p.m. for 15 min as described previously.[15] An enzyme-linked immunosorbent assay, from Millipore (IMM001, Billerica, MA) was used to measure mast cell activation, according to the manufacturer's recommendations.

Mast cell reconstitution and staining in peripheral tissues

Bone marrow cells were harvested from 6- to 8-week-old WT mice. Cells were filtered, spun, red blood cells were then lysed, and the supernatant discarded. Cells were cultured in RPMI (Sigma-Aldrich) using 15% fetal calf serum, 1% Pen/Strep, 2 mmol/l L-glutamine, 1 mmol/l sodium pyruvate, and 50 μm 2-M,E. Interleukin-3 (from WEHI3 cell culture supernatants) and 12.5 ng/ml recombinant mouse stem cell factor (R&D Systems) were added. Culture media were changed every 3 days. After 8 weeks, mast cell purity (>98%) was assessed using a cyto-spinner after toluidine blue staining. A total of 5×10^6 cells were injected intravenously into the mice. We waited 12 weeks for full re-constitution to develop.[14] Mast cells were identified by staining lymph nodes and kidneys with toluidine blue after fixation in methyl Carnoy's solution. Reconstitution was confirmed by staining for mast cells with toluidine blue in peripheral tissues and kidneys as described previously.[15] To demonstrate that mast cells are recruited early to the obstructed kidney, we labeled mature mast cells, after 8 weeks of culture with a CellTracker (CMTPX) from Invitrogen (Newcastle, New South Wales, Australia), this was dissolved in dimethylsulfoxide to a concentration of 10 mmol/l. Cells (30×10^6) were stained with 20 μm CMPTX and incubated for 30 min at 30 °C, spun (12,000 r.p.m. for 7 min), and resuspended in isotonic saline. Labeled mast cells (1×10^6) were injected subcutaneously into the base of tail of $Kit^{W\text{-}sh/W\text{-}sh}$ mice. We then performed unilateral ureteric ligation and removed the hydronephrotic and contralateral kidneys, 6 h later. Kidney sections were viewed under immunofluorescent light, Leica (Leica Microsystems, Wetzlar, Germany) D300F using a filter 13, and images captured using Adobe Photoshop.

DISCLOSURE

All the authors declared no competing interests.

ACKNOWLEDGMENTS

SAS is supported by a Jacquot Research Establishment Award administered by the Royal Australasian College of Physicians. SRH is supported by a National Medical Research Council of Australia project grant.

SUPPLEMENTARY MATERIAL

Figure 1. Increased macrophages and CD4 + T cells were seen in the hydronephrotic kidneys of WT mice compared to $Kit^{W\text{-}sh/W\text{-}sh}$ mice, 7 days after UUO.

Supplementary material is linked to the online version of the paper at http://www.nature.com/ki

REFERENCES

1. Kuncio GS, Neilson EG, Haverty T. Mechanisms of tubulointerstitial fibrosis. *Kidney Int* 1991; **39**: 550–556.
2. Harris RC, Neilson EG. Toward a unified theory of renal progression. *Annu Rev Med* 2006; **57**: 365–380.
3. Zeisberg M, Neilson EG. Mechanisms of tubulointerstitial fibrosis. *J Am Soc Nephrol* 2010; **21**: 1819–1834.
4. Miyajima A, Chen J, Lawrence C *et al.* Antibody to transforming growth factor-beta ameliorates tubular apoptosis in unilateral ureteral obstruction. *Kidney Int* 2000; **58**: 2301–2313.
5. Yokoi H, Mukoyama M, Nagae T *et al.* Reduction in connective tissue growth factor by antisense treatment ameliorates renal tubulointerstitial fibrosis. *J Am Soc Nephrol* 2004; **15**: 1430–1440.
6. Bascands JL, Schanstra JP. Obstructive nephropathy: insights from genetically engineered animals. *Kidney Int* 2005; **68**: 925–937.
7. Tapmeier TT, Fearn A, Brown K *et al.* Pivotal role of CD4+ T cells in renal fibrosis following ureteric obstruction. *Kidney Int* 2010; **78**: 351–362.
8. Ma FY, Liu J, Kitching AR *et al.* Targeting renal macrophage accumulation via c-fms kinase reduces tubular apoptosis but fails to modify progressive fibrosis in the obstructed rat kidney. *Am J Physiol Renal Physiol* 2009; **296**: F177–F185.
9. Holdsworth SR, Summers SA. Role of mast cells in progressive renal diseases. *J Am Soc Nephrol* 2008; **19**: 2254–2261.
10. Marshall JS. Mast-cell responses to pathogens. *Nat Rev Immunol* 2004; **4**: 787–799.
11. Lu LF, Lind EF, Gondek DC *et al.* Mast cells are essential intermediaries in regulatory T-cell tolerance. *Nature* 2006; **442**: 997–1002.
12. Echtenacher B, Mannel DN, Hultner L. Critical protective role of mast cells in a model of acute septic peritonitis. *Nature* 1996; **381**: 75–77.
13. Malaviya R, Ikeda T, Ross E *et al.* Mast cell modulation of neutrophil influx and bacterial clearance at sites of infection through TNF-alpha. *Nature* 1996; **381**: 77–80.
14. Grimbaldeston MA, Chen CC, Piliponsky AM *et al.* Mast cell-deficient W-sash c-kit mutant Kit W-sh/W-sh mice as a model for investigating mast cell biology *in vivo*. *Am J Pathol* 2005; **167**: 835–848.
15. Summers SA, Chan J, Gan PY *et al.* Mast cells mediate acute kidney injury through the production of TNF. *J Am Soc Nephrol* 2011; **22**: 2226–2236.
16. Scandiuzzi L, Beghdadi W, Daugas E *et al.* Mouse mast cell protease-4 deteriorates renal function by contributing to inflammation and fibrosis in immune complex-mediated glomerulonephritis. *J Immunol* 2010; **185**: 624–633.
17. Mack M, Rosenkranz AR. Basophils and mast cells in renal injury. *Kidney Int* 2009; **76**: 1142–1147.
18. Timoshanko JR, Kitching AR, Semple TJ *et al.* A pathogenetic role for mast cells in experimental crescentic glomerulonephritis. *J Am Soc Nephrol* 2006; **17**: 150–159.
19. Hochegger K, Siebenhaar F, Vielhauer V *et al.* Role of mast cells in experimental anti-glomerular basement membrane glomerulonephritis. *Eur J Immunol* 2005; **35**: 3074–3082.
20. Kanamaru Y, Scandiuzzi L, Essig M *et al.* Mast cell-mediated remodeling and fibrinolytic activity protect against fatal glomerulonephritis. *J Immunol* 2006; **176**: 5607–5615.
21. Eller K, Wolf D, Huber JM *et al.* IL-9 production by regulatory T cells recruits mast cells that are essential for regulatory T cell-induced immune suppression. *J Immunol* 2011; **186**: 83–91.
22. Hakonarson H, Carter C, Kim C *et al.* Altered expression and action of the low-affinity IgE receptor FcepsilonRII (CD23) in asthmatic airway smooth muscle. *J Allergy Clin Immunol* 1999; **104**: 575–584.
23. Margulis A, Nocka KH, Brennan AM *et al.* Mast cell-dependent contraction of human airway smooth muscle cell-containing collagen gels: influence of cytokines, matrix metalloproteases, and serine proteases. *J Immunol* 2009; **183**: 1739–1750.
24. Li Y, Zhou L, Liu F *et al.* Mast cell infiltration is involved in renal interstitial fibrosis in a rat model of protein-overload nephropathy. *Kidney Blood Press Res* 2010; **33**: 240–248.
25. Blank U, Essig M, Scandiuzzi L *et al.* Mast cells and inflammatory kidney disease. *Immunol Rev* 2007; **217**: 79–95.
26. Gordon JR, Galli SJ. Promotion of mouse fibroblast collagen gene expression by mast cells stimulated via the Fc epsilon RI. Role for mast cell-derived transforming growth factor beta and tumor necrosis factor alpha. *J Exp Med* 1994; **180**: 2027–2037.
27. Li MO, Wan YY, Sanjabi S *et al.* Transforming growth factor-beta regulation of immune responses. *Annu Rev Immunol* 2006; **24**: 99–146.
28. Pennington DW, Lopez AR, Thomas PS *et al.* Dog mastocytoma cells produce transforming growth factor beta 1. *J Clin Invest* 1992; **90**: 35–41.
29. Lindstedt KA, Wang Y, Shiota N *et al.* Activation of paracrine TGF-beta1 signaling upon stimulation and degranulation of rat serosal mast cells: a novel function for chymase. *FASEB J* 2001; **15**: 1377–1388.
30. Gruber BL, Marchese MJ, Kew RR. Transforming growth factor-beta 1 mediates mast cell chemotaxis. *J Immunol* 1994; **152**: 5860–5867.
31. Olsson N, Piek E, ten Dijke P *et al.* Human mast cell migration in response to members of the transforming growth factor-beta family. *J Leukocyte Biol* 2000; **67**: 350–356.
32. Sirvent AE, Gonzalez C, Enriquez R *et al.* Serum tryptase levels and markers of renal dysfunction in a population with chronic kidney disease. *J Nephrol* 2010; **23**: 282–290.
33. Matute-Bello G, Wurfel MM, Lee JS *et al.* Essential role of MMP-12 in Fas-induced lung fibrosis. *Am J Respir Cell Mol Biol* 2007; **37**: 210–221.
34. Ramos L, Pena G, Cai B *et al.* Mast cell stabilization improves survival by preventing apoptosis in sepsis. *J Immunol* 2010; **185**: 709–716.
35. Lange-Sperandio B, Trautmann A, Eickelberg O *et al.* Leukocytes induce epithelial to mesenchymal transition after unilateral ureteral obstruction in neonatal mice. *Am J Pathol* 2007; **171**: 861–871.
36. Henderson NC, Mackinnon AC, Farnworth SL *et al.* Galectin-3 expression and secretion links macrophages to the promotion of renal fibrosis. *Am J Pathol* 2008; **172**: 288–298.
37. Margulis A, Nocka KH, Wood NL *et al.* MMP dependence of fibroblast contraction and collagen production induced by human mast cell activation in a three-dimensional collagen lattice. *Am J Physiol Lung Cell Mol Physiol* 2009; **296**: L236–L247.
38. Helske S, Syvaranta S, Kupari M *et al.* Possible role for mast cell-derived cathepsin G in the adverse remodelling of stenotic aortic valves. *Eur Heart J* 2006; **27**: 1495–1504.
39. Yang FC, Chen S, Clegg T *et al.* Nf1 ± mast cells induce neurofibroma like phenotypes through secreted TGF-beta signaling. *Hum Mol Genet* 2006; **15**: 2421–2437.
40. Wang HW, Tedla N, Hunt JE *et al.* Mast cell accumulation and cytokine expression in the tight skin mouse model of scleroderma. *Exp Dermatol* 2005; **14**: 295–302.
41. Jeong DH, Lee GP, Jeong WI *et al.* Alterations of mast cells and TGF-beta1 on the silymarin treatment for CCl(4)-induced hepatic fibrosis. *World J Gastroenterol* 2005; **11**: 1141–1148.
42. Soga Y, Takai S, Koyama T *et al.* Attenuating effects of chymase inhibitor on pericardial adhesion following cardiac surgery. *J Card Surg* 2007; **22**: 343–347.
43. Kim DH, Moon SO, Jung YJ *et al.* Mast cells decrease renal fibrosis in unilateral ureteral obstruction. *Kidney Int* 2009; **75**: 1031–1038.
44. Zhou JS, Xing W, Friend DS *et al.* Mast cell deficiency in Kit(W-sh) mice does not impair antibody-mediated arthritis. *J Exp Med* 2007; **204**: 2797–2802.
45. Jones LK, O'Sullivan KM, Semple T *et al.* IL-1RI deficiency ameliorates early experimental renal interstitial fibrosis. *Nephrol Dial Transplant* 2009; **24**: 3024–3032.
46. Summers SA, Steinmetz OM, Li M *et al.* Th1 and Th17 cells induce proliferative glomerulonephritis. *J Am Soc Nephrol* 2009; **20**: 2518–2524.
47. Summers SA, Phoon RK, Ooi JD *et al.* The IL-27 receptor has biphasic effects in crescentic glomerulonephritis mediated through Th1 responses. *Am J Pathol* 2011; **178**: 580–590.